

Numerical Simulation of Combustion Behavior in 6.9 m Sintered Brick Tunnel Kiln

Ning Xu¹, Yunfei Yan¹, Yue Xu^{2*}

¹Key Laboratory for Advanced Technology in Environmental Protection of Jiangsu Province, Yancheng Institute of Technology, Yancheng 224051, China

²School of Materials, The University of Manchester, Manchester, M139PL, UK

Abstract: Using fluid dynamic software, geometric model, of which the mesh generation was performed with hybrid grids, was established according to the actual structure of the firing zone of a company's sintered brick tunnel kiln. The standard k- ϵ model, species transport, finite-rate chemistry model and pollutant formation model were used to simulate the section temperature of firing zone and the concentration change of NO in the kiln at different load porosity, thus to give reference for the furnace design, arrangement of bricks and NO emission control. The simulation results showed that: with the increase of the load porosity, the region temperature of the load gradually increased; the gap region temperature between the load and kiln roof gradually decreased first. When the porosity reached 0.6, the temperature dropped to the lowest, and then rose slowly. The NO concentration in the section located between the load and kiln roof decreased first, then increased, and decreased again.

Key word: Numerical simulation, sintered brick tunnel kiln, NO concentration

1 Introduction

Tunnel kiln as a continuous counter flow operation thermal equipment was widely used in the sintered brick industry. The manufacturing process of sintered brick tunnel kiln can be simply described as follows: First, dried green bricks with a certain moisture content are loaded on the kiln car from the head kiln into the kiln, passed through the preheating zone and heated by the high temperature flue gas from the firing zone. Then, the product enters into the firing zone. The flames and gas produced by the fuel are heated directly on the green bricks to reach a certain temperature, and physical&chemical reactions occur. Later, the products enter into the cooling zone. The heat is transferred to the cold air blowing from the kiln back end. The product itself reduces to a certain temperature and come out of the kiln end .This process forms a firing cycle.

*Corresponding author: Email: eeyuexu@126.com

Tunnel kiln firing process requires a lot of energy and produces a great deal of gas and dust pollutants [1-3]. Therefore, studying its combustion process and seeking the way to reduce energy consumption and control pollutant emission quantity have practical significance. However, because of the complex structure and bulky volume of the tunnel kiln, direct experimental studies are expensive and time-consuming. The development of computer technology enables the thermal process of tunnel kiln for direct simulation on computer to become a reality. The commercial software at home and abroad has been used for a lot of tunnel kiln numerical simulation in recent years. Nicolau and Ddam [4] established a numerical model to simulate the energy balance during the sintered brick process of tunnel kiln. The energy consumption conditions of kiln walls were studied with and without insulation layer, and the energy consumption were reduced by more than 10% with insulation layer. Santos [5] proposed a mathematical formula to analyze the heat transfer between different components of tunnel kiln. Timber and natural gas were used as fuel for the thermal process simulation of tunnel kiln, respectively. The results were compared with the experiment data and it was found that the numerical simulation well reflected the actual heat distribution and transport phenomena of tunnel kiln. Oba and Possamai [6] used the numerical simulation method to analyze the tunnel kiln production process of roofing tile. The results were compared with experimental results. Cheng Zeng [7] used Fluent software to simulate oxygen-enriched combustion process in firing zone of tunnel kiln. With the increase of oxygen mass fraction, the temperature field in the kiln was more and more uniform, and the NO concentration of exit section increased. But the increase rate gradually decreased, and unit integrated energy consumption of the product reduced.

In this paper, computational fluid dynamic simulation software Fluent was used to simulate the combustion process of firing zone of the sintered brick tunnel kiln, analyze the effect of different load porosity on temperature distribution in the kiln and NO concentration, and explore pollutant emission control methods of the tunnel kiln.

2 Geometric Modeling of Firingzone in Tunnel Kiln

According to the tunnel kiln with the size of 105*6.9m in an enterprise of Jiangsu province, the cross section structure diagram of firingzone in tunnel kiln is shown in Fig.1. The main structures of tunnel kiln include: kiln roof, kiln wall, load support, kiln car, and kiln burner at the top of the kiln roof. Load was fabricated on the cushion, and a certain gap was maintained between load and kiln wall as well as kiln roof. The kiln wall and kiln roof play roles in refractory and thermal insulation. The fuel and air were injected into the kiln through the kiln burner, and the generated high-temperature gas was used to heat the load.

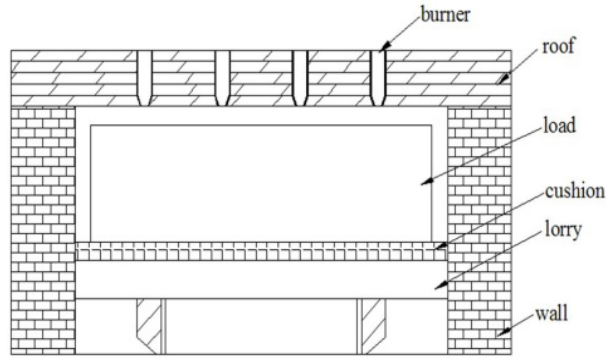


Figure 1: Main components of the firing zone section

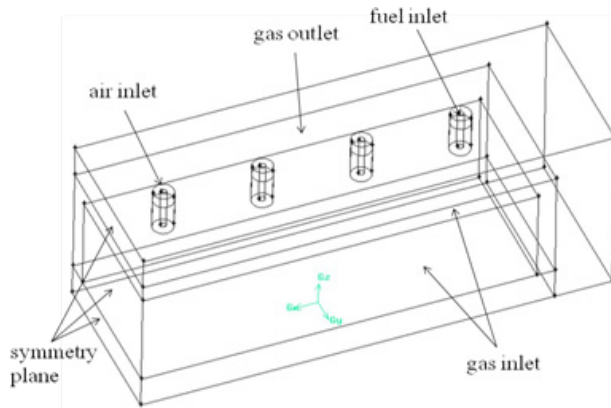


Figure 2: Geometric model of a segment firing zone

In this paper, we studied the tunnel kiln, in which the width of cross section was 6.9 m, the distance between cushion and kiln roof was 1.2 m, the distance between load and kiln roof was 0.15 m, and eight kiln burners were symmetrically dispersed on the top of kiln roof. In order to save computational resources, half of the cross section in the part of firing zone was used as the geometry model. The geometry model is shown as Fig.2.

3 Mathematical Models

The standard K-ε model, species transport model and NO_x pollutant model were solved in order to simulate the temperature field and the NO concentration in the firing zone of tunnel kiln. The following assumptions were adopted for the model: (a) the fluid accorded with the ideal gas law; (b) it was considered as continuous and incompressible medium; (c) the load was set for porous media; (d) all solid areas were considered to be isotropic and had a constant physical properties; (e) solid wall was set as impermeable and non-slipping boundary condition.

3.1 Governing equation

(1) The conservation equation of mass

$$\frac{\partial \rho}{\partial t} + \frac{\partial}{\partial x_i} (\rho u_i) = 0 \quad (1)$$

Where ρ is the density, u is the velocity.

(2) The conservation equation of momentum (N-S equation)

$$\frac{\partial}{\partial t} (\rho u_i) + \frac{\partial}{\partial x_j} (\rho u_i u_j) = -\frac{\partial p}{\partial x_i} + \frac{\partial}{\partial x_j} \left[\mu \left(\frac{\partial u_i}{\partial x_j} + \frac{\partial u_j}{\partial x_i} - \frac{2}{3} \delta_{ij} \frac{\partial u_k}{\partial x_k} \right) \right] + \frac{\partial}{\partial x_j} (-\rho \overline{u_i u_j}) \quad (2)$$

Where P is the pressure, μ is the viscosity of fluid.

(3) The conservation equation of energy

$$\text{div}(\rho v h) = \text{div} \left[\left(\frac{\mu}{Pr} \right) \text{grad} h \right] + v \cdot \text{grad} \rho + S_h \quad (3)$$

Where $Pr = \mu c_p / k$ is the Prandtl constant, S_h is the heat resource including chemical reaction heat generation, convection heat transfer, radiation heat transfer and any other heat resources defined by the user.

Enthalpy of the equation is defined as:

$$h = \int_{T_{ref}}^T C_p dT \quad (4)$$

Where $T_{ref} = 298.15K$.

3.2 NO pollutant generation model

The generating mechanism of NO mainly includes "thermal-typed", "promote-typed" and "fuel-typed". When the fuel is liquid or solid, a high promotion of pollutant is fuel-typed NO. Under the condition of gaseous fuel, few fuel-typed NO was generated. In this article, we used the natural gas as fuel. So the major concerns are "thermal-typed" and "promote-typed" NO. The NO transport equation is given by:

$$\frac{\partial}{\partial t} (\rho Y_{NO}) + \nabla \cdot (\rho \bar{v} Y_{NO}) = \nabla \cdot (\rho D \nabla Y_{NO}) + S_{NO} \quad (5)$$

Where ρ_{no} is the density of NO, it changes with the variation of temperature and concentration of other components.

(1) Thermal-typed NO: the nitrogen was oxidized to the NO at high temperature, and it was called thermal-typed NO. The main reaction equation is described as follows:



The generation of thermal-typed NO is calculated according to the following equation:

$$\frac{d[NO]}{dt} = 2k_{f,1}[O][N_2] \frac{\left(1 - \frac{k_{r,1}k_{r,2}[NO]^2}{k_{f,1}[N_2]k_{f,2}[O_2]}\right)}{\left(1 + \frac{k_{r,1}[NO]}{k_{f,2}[O_2] + k_{f,3}[OH]}\right)}$$

$$k_{f,1} = 1.8 \times 10^8 e^{-38370/T} \quad k_{r,1} = 3.8 \times 10^7 e^{-425/T} \quad (6)$$

$$k_{f,2} = 1.8 \times 10^4 T e^{-4680/T} \quad k_{r,2} = 3.81 \times 10^3 T e^{-20820/T}$$

$$k_{f,3} = 7.1 \times 10^7 e^{-450/T}$$

Where $[O_2]$, $[N_2]$, $[OH]$, $[NO]$ are the concentration of O_2 , N_2 , OH and NO , T is the kelvin temperature, t is the time.

(2) Promote-typed NO: The NO was generated on the flame when hydrocarbons burned under the condition of low oxygen concentration, It was produced through a series of complex chemical reactions.

The main influence factors of the thermal NO generation is the chemical reaction which involved the CH pyrolyzed from the fuel. The governing equations of the thermal-typed NO production rate can be described as:

$$\frac{d[NO]}{dt} = k[CH][N_2] \quad (7)$$

3.3 Boundary Condition

The circular channel in the middle of the burner was defined as the fuel inlet and the annular channel around the fuel inlet was defined as the air inlet .Both of the fuel inlet and the air inlet were velocity inlet. The gas inlet was set for velocity inlet and the gas outlet set for the pressure outlet. The kiln wall and roof were defined as couple wall .The load area was considered as porosity.

3.4 Model Solving Method

The Tet/Hybrid grid was used to mesh the kiln body, kiln car, burner, load and the kiln wall.

The total amount of grids was 501309. The finite volume method was adopted to discrete the governor equation and the second up wind method was used to solve the conservation equation of momentum and the conservation equation of energy. Iteration was done until convergence was reached.

4 Results and Discussions

4.1 Temperature distribution of the cross section when the porosity of the load is 0.6.

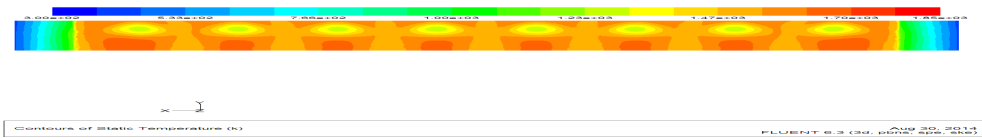


Figure 3: temperature field for section $Z=0.75$

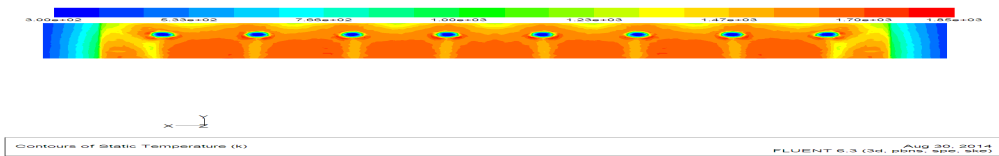


Figure 4: temperature field for section $Z=1.28$

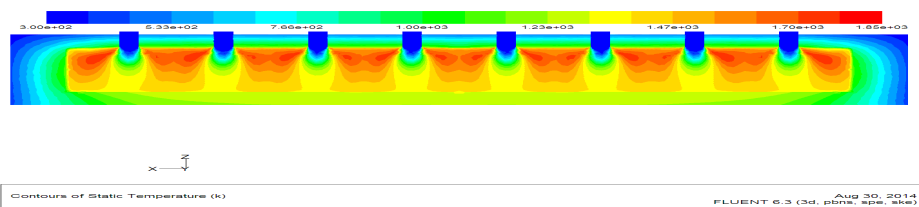


Figure 5: Temperature field for section $Y=0$

Fig. 3, 4, and 5 show the temperature distribution contours of the section $Z = 0.75$, $Z = 1.28$ and $Y = 0$, respectively. The section of $Z = 0.75$ is the across load area. The section of $Z = 1.28$ is the located area in the gap between the load and kiln roof, and the section of $Y = 0$ is the across area between load and the center of the burner. The combustion of fuel and air produces hot gas to heat the load, and heat is lost from the bottom of the kiln car and the external surface of the kiln wall and roof. It can be observed from these figures: (1) the high temperature area is focused on the gap between the load and the kiln roof. The reason is that the contact of fuel and air are hindered by the load when they are injected into the kiln. Then, strong turbulence takes place in this area, and the fuel and air are mixed thoroughly and burned fiercely, forming high temperature zone. The high temperature area can result

in uneven temperature distribution and increases kiln refractory consumption. Therefore, this gap should be minimized. (2) The low temperature region is located at the area where the fuel and air are injected, which is caused by the high speed injection of cool fuel and air. More uniform temperature distribution will be got if the fuel is preheated before injection.

4.2 The average temperature and NO concentration of each section with different load porosity

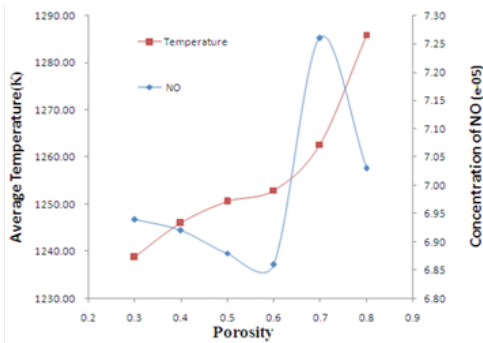


Fig. 6 The average temperature and concentration of NO in the section of Y=0 with different porosity

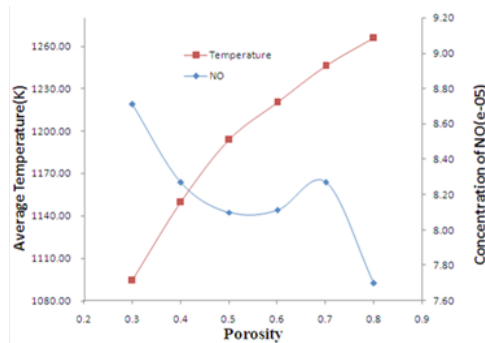


Fig. 7 The average temperature and concentration of NO in the section of Z=0.75 with different porosity

Fig. 6 and 7 show the change of average temperature and NO concentration in the section of Y=0 and Z=0.75 when the porosity of load changes from 0.3 to 0.8. As the porosity increases, the turbulence of gas in the load area becomes intense and burns fiercely. So the temperature rises gradually. When porosity of the load increases from 0.3 to 0.6, the temperature distribution of kiln becomes more uniform, and the local high-temperature area reduces. So the NO concentration decreases. When the porosity increases to 0.7, the average temperature rises and NO concentration increases due to the fierce burning. When the porosity increases to 0.8, the average temperature continues to rise. But the NO concentration in this section becomes lower because the load arrangement is very sparse, and gas's velocity is larger, and these make the produced NO flow to the next region of kiln.

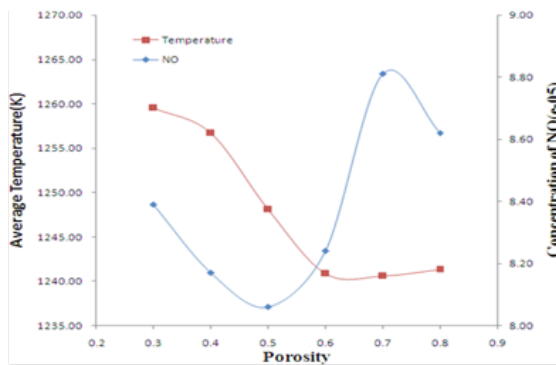


Fig. 8 The average temperature and concentration of NO in the section of Z=1.28 with different porosity

Fig. 8 shows the changes of average temperature and NO concentration at Z = 1.28

section when the porosity of load increases from 0.3 to 0.8. As the porosity is low, bricks are arranged compact, so the fuel and air are hindered by the load. Fuel burns in the gap between load and kiln roof, and then the temperature of this section rises. With the increase of porosity and decrease of resistance, more gas is involved into the load area, and the temperature of the section decreases. When the porosity increases to 0.6, the temperature rises slowly. The variation trend of NO concentration is the same as that when $Y = 0$, $Z = 0.75$ with the increase of porosity.

5 Conclusion

In this paper, fluid dynamic software Fluent was used to simulate the combustion section temperature distribution of tunnel kiln and NO concentration changes with different porosity of the load. Three sections of $Y = 0$, $Z = 0.75$ and $Z = 1.28$ were analyzed, and the results are as follows:

(1) Because the injected fuel and air was hindered by the load, a certain high temperature region was formed in the gap between the load and kiln roof. The hot gas of this region did not directly heat the load to cause the section temperature difference of height direction in kiln and energy waste. So this gap should be reduced as possible.

(2) With the increase of the load porosity, the flame will be easier to enter the load interior, and the temperature of the section in load region increased gradually. The temperature of gap area between the load and kiln roof gradually decreased first. When the porosity reached 0.6, the temperature dropped to the lowest. Then the temperature increased slowly with the porosity changed from 0.6 to 0.8 due to the influence of the load region temperature increase.

(3) With the increase of the load porosity, NO concentration changed in the same trend in each section. The NO concentration gradually decreased at 0.3-0.5, increased at 0.6-0.7, and then decreased gradually over 0.7. The NO concentration reached to lower values at 0.5-0.6 and 0.8. The excessively large porosity will result in lower yields. So a porosity of 0.5 was considered to be optimal when thinking about the NO concentration.

(4) With the increase of load porosity, the load temperature and temperature uniformity in the kiln increased, helping to improve product quality. However, the increase of porosity will reduce the tunnel kiln production, so the best porosity choice must be considered comprehensively.

Acknowledgements

Financial support of the work by the National Key Technology R&D Program of China (Grant no. 2013BAC13B01) is greatly acknowledged.

References

- [1] Sinem Kaya, Ebru Manchan. Modeling and optimization of the firing zone of a tunnel kiln to predict the optimal feed locations and mass fluxes of the fuel and secondary air. *Applied Energy*, 2009, 86: 325-332.
- [2] Ebru Mancuhan, Kurtul Kucukada. Optimization of fuel and air use in a tunnel kiln to produce coal admixed bricks, *Applied Thermal Engineering*. 2006, 26:1556-1563.
- [3] G.HALÁSZ, J. TÓTH . Energy-optimal operation conditions of a tunnel kiln. *Comput. chem. Engng*, 1988, 12:183-187.
- [4] V.P. Nicolau, A.P. Dadam. Numerical and experimental thermal analysis of a tunnel kiln used in ceramic production. *Journal of the Brazilian Society of Mechanical Sciences & Engineering*, 2009, 4:297-304.
- [5] Santos, G.M. Study of thermal behavior of a tunnel kiln used in red ceramic industry. Master Thesis, *Federal University of Santa Catarina, Santa Catarina, Brazil*. 2001.
- [6] R.Oba, T.S.Possamai. Thermal analysis of tunnel kiln used to produce roof tiles. *Applied Thermal Engineering*, 2014, 63: 59-65.
- [7] Cheng Zeng. The simulating of Gas Oxygen-enrichment combustion in tunnel kiln. Master Thesis, *Huazhong University of Science & Technology*, 2012.